Heliyon 10 (2024) e27481

Contents lists available at ScienceDirect

Heliyon

journal homepage: www.cell.com/heliyon

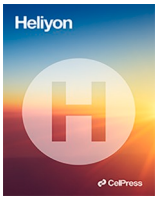

Review article

Reliability of MEMS inertial devices in mechanical and thermal environments: A review

Yingyu Xu [a,c], Shuibin Liu [a], Chunhua He [a,*], Heng Wu [a], Lianglun Cheng [a], Guizhen Yan [b], Qinwen Huang [c,**]

[a] School of Computer, Guangdong University of Technology, Guangzhou, 510006, China
[b] National Key Laboratory of Science and Technology on Micro/Nano Fabrication, Institute of Microelectronics, Peking University, Beijing, 100871, China
[c] Science and Technology on Reliability Physics and Application of Electronic Component Laboratory, China Electronic Product Reliability and Environmental Testing Research Institute, Guangzhou, 510000, China

ARTICLE INFO

Keywords:
MEMS inertial devices
Thermal reliability
Mechanical reliability
Multiphysics coupling
Failure modes and mechanisms

ABSTRACT

The reliability of MEMS inertial devices applied in complex environments involves interdisciplinary fields, such as structural mechanics, material mechanics and multi-physics field coupling. Nowadays, MEMS inertial devices are widely used in the fields of automotive industry, consumer electronics, aerospace and missile guidance, and a variety of reliability issues induced by complex environments arise subsequently. Hence, reliability analysis and design of MEMS inertial devices are becoming increasingly significant. Since the reliability issues of MEMS inertial devices are mainly caused by complex mechanical and thermal environments with intricate failure mechanisms, there are fewer reviews of related research in this field. Therefore, this paper provides an extensive review of the research on the reliability of typical failure modes and mechanisms in MEMS inertial devices under high temperature, temperature cycling, vibration, shock, and multi-physical field coupling environments in the last five to six years. It is found that though multiple studies exist examining the reliability of MEMS inertial devices under single stress, there is a dearth of research conducted under composite stress and a lack of systematic investigation. Through analyzing and summarizing the current research progress in reliability design, it is concluded that multi-physical field coupling simulation, theoretical modeling, composite stress experiments, and special test standards are important directions for future reliability research on MEMS inertial devices.

1. Introduction

Micro-electro-mechanical systems (MEMS) are designed to achieve specific sensor or actuator functions and are integrated systems fabricated on a microscale [1,2]. Nowadays, MEMS technology has become extensively used in the civil and military sectors, with inertial measurement being among the most vital application areas. Commonly used inertial devices comprise MEMS gyroscopes, MEMS accelerometers, and MEMS magnetometers. They are applied to gauge the angular rate, acceleration, and magnetic field

* Corresponding author.
** Corresponding author.
E-mail addresses: hechunhua@pku.edu.cn (C. He), 971230012@163.com (Q. Huang).

https://doi.org/10.1016/j.heliyon.2024.e27481
Received 28 May 2023; Received in revised form 29 February 2024; Accepted 29 February 2024
Available online 3 March 2024

intensity, correspondingly [3,4].

MEMS inertial devices can be used in smartphones, wearable devices, unmanned aerial vehicles, the automotive industry, aerospace, and missile guidance owing to their small size, low power consumption, superior performance, and low cost, which have garnered increasing attention from researchers worldwide [5]. Currently, MEMS inertial devices, particularly gyroscopes and accelerometers, have undergone rapid development and commercialization [6]. With the wide adoption of MEMS inertial devices, they are inevitably exposed to various harsh operating environments. Although vacuum encapsulation technology effectively mitigates the impact of the external factors on MEMS devices, excessive stress loads might cause gas leakage from the encapsulation, leading to increased air pressure, quality factor degradation, and ultimately structural failure. Severe vibration, shock, and thermal impacts may also result in fatigue, fracture, delamination, particle contamination and other issues [7,8]. The main failure modes of MEMS inertial devices under external environmental loads are summarized in Table 1.

MEMS inertial devices are susceptible to the failures mentioned above, regardless of whether they are used militarily or commercially. Component failure of the devices can lead to detection data errors, system breakdowns, and increased maintenance expenses, all of which would have a serious impact on product applications. Therefore, improving the reliability of MEMS inertial devices under various complex environmental stresses is the key to maintaining performance and extend-ing product survival. Reliability design mainly involves structural optimization, circuit design, reliability modelling and analysis, reliability characterization and life prediction. There are currently numerous reports on the reliability of integrated circuits, while there are relatively few reports related to the reliability of MEMS inertial devices, and no review of research on MEMS inertial devices in complex mechanical and high-temperature environments has been reported. In this paper, the current state of research in this field is thoroughly investigated to summarize the influences of complex mechanical and high-temperature coupling environments on MEMS inertial devices and to discuss the future research trends and challenges, which are of great significance to the development of MEMS reliability.

The search strategies for this paper include: (a) searching the relevant data from the digital databases, such as Google Scholar, IEEE, ScienceDirect and IOP; (b) investigating the relevant data from companies, research institutes and so on. The inclusion criteria are that the relevant contents are related to the theme of reliability research on MEMS inertial devices. The keywords or terms include MEMS inertial device, gyroscope, accelerometer, reliability, failure, shock or impact, vibration, temperature or thermal, etc., and the published time is from 2018 to 2023. In terms of the summary method, the cited papers are classified according to different environmental stresses, such as vibration, impact, and thermal stress. Since the relevant data are limited, the narrative method instead of the statistical method is adopted for the summary of this review. Besides, the conclusion made in this article may be biased. However, we have tried our best to reduce the risk by investigating and summarizing the relevant papers as much as possible.

1.1. MEMS reliability with consideration of vibration

In general, MEMS inertial devices are utilized within the automotive industry, aerospace, and missile guidance for attitude stabilisation and positioning navigation [10]. Industrial-grade gyroscopes are usually exposed to random vibrations ranging from 50 Hz to 2 kHz, with a total root mean square (RMS) of 6–20 g. Military gyroscopes, on the other hand, are subject to random vibrations from 0 to 10 kHz, with a total RMS of 20–30 g [11]. Vibration is one of the most important factors affecting the reliability of MEMS inertial devices. The following is a comprehensive overview of the research advancements in the reliability of MEMS inertial devices under vibration.

1.2. Typical vibration failure modes

According to the literature [12,13], the main failure modes of MEMS inertial devices when subjected to vibration stress are fatigue, adhesion, stiffness degradation, pull-in instability, and structural fracture.

MEMS gyroscopes are applied to measure the angular rate based on the Coriolis effect. Accordingly, the velocity of the drive mode must be maintained constant, which means that the moving structure should oscillate at a constant amplitude. If external forces are applied, increasing the amplitude of structural vibrations over an extended period, the spring beams may suffer from material fatigue and ultimately fracture. Yao Liu et al. [14] discovered that numerous polycrystalline silicon materials utilized in MEMS devices displayed crack defects. These defects are speculated to have arisen during the processing of silicon wafers, which involves heat treatment, etching, dicing, and more. The stress concentrations tend to emerge at crack defects under intense vibration loads, thus resulting in the fracture failure at the point of intersection between inclined and parallelogram beams, as shown in Fig. 1.

Table 1
Main failure modes of MEMS inertial devices in relation to external environmental loads [9].

	vibration	shock	temperature
fracture	✓	✓	✓
fatigue	✓		✓
creep		✓	
adhesion	✓	✓	
wear	✓	✓	
delamination		✓	✓
contamination	✓	✓	
short circuit	✓	✓	

Elastic beams of a MEMS inertial device constantly undergo repeated mechanical motion with high-vibration load cycles. The resulting alternating stress is likely to cause fatigue damage in the structure, which makes the stiffness of the structure decrease, causes performance degradation, and eventually causes fatigue fracture.

Ebiakpo Kakandar et al. [15] investigated the effect of driving a MEMS resonator at its resonant frequency by supplying a high sinusoidal voltage to its comb structure. As shown in Fig. 2, when the rotation amplitudes are large enough (greater than 14 mrad, equivalent to stress amplitudes exceeding 300 MPa), the driving of the microresonator leads to cyclic mechanical motion of the microbeam sidewalls in the form of compression and tension, resulting in fatigue damage and crack propagation or even fracture. This fatigue phenomenon is exacerbated especially under random vibration conditions.

Due to the continuous accumulation of fatigue damage in the polycrystalline silicon microbeam, the material properties gradually degrade. Once the mechanical recovery force of the material is less than the electrostatic driving force, the suspension beams will collapse towards the fixed electrode, and the adhesion failure occurs. Shun Zhang and Jin Zhang [16] studied this phenomenon and demonstrated that with increasing vibration amplitude, the rate of fatigue also increased, resulting in pull-in instability. For the fatigue-induced pull-in instability, Tajalli et al. [17] applied the wavelet transform algorithm based on the Gabor function to calculate the damage in the microstructure and investigated the mechanism of surface cracks. The structural model of the pull-in instability is shown in Fig. 3. In conclusion, increasing crack depth results in lower pull-in voltages. As the crack position approaches the fixed endpoints, the pull-in voltage drops significantly.

As MEMS structures have an extremely small mass and a large specific surface area, distances between combs or microbeams become extremely small under high vibrational stress, resulting in various surface effects. Because of adhesion forces (capillary, van der Waals, and electrostatic forces), a short-circuit failure or impaired function would occur when two surfaces make contact. By using a stopper or a limiting structure, it enables MEMS gyroscopes to avoid the problems associated with structural pull-in and adhesion resulting from vibrations.

1.3. Vibration failure mechanisms

Large vibration loads cause various failures in microbeams and metal leads, such as fatigue and fracture. Therefore, it is essential to analyze the vibration response of curved leads or microbeams to understand the vibration failure mechanism.

The vibration response characteristics and intrinsic frequencies of metal leads were derived in detail based on the Euler-Bernoulli beam theory and Hamilton's principle [18]. It was determined that when the external acceleration frequency aligns with the natural frequency of the gold wire, resonance and stress concentration would result in fracture failure. Yunbo Shi et al. [19] modeled the vibration of two- and three-degree-of-freedom systems and calculated the first-order natural frequency of an accelerometer as a function of material parameters using MATLAB. The model indicated that the first-order natural frequency of the accelerometer was strongly dependent on the material parameters. The first-order natural frequency could be increased by improving the packaging material to avoid resonance, thus improving the vibration resistance.

The analytical model for the resonant frequency of a butterfly gyroscope in the drive mode was deduced by Yao Liu. With the increase in vibration time, residual stresses in the silicon structure would slowly deteriorate the device's performance since resonant frequency and mechanical sensitivity would gradually decrease [20]. This result was consistent with the result of modal analysis by the Finite Element Method (FEM). For the application environment, Wenhao Luo et al. [21] proposed a method for measuring the vibration characteristics of MEMS microstructures in vacuum, high- and low-temperature environments. This method provides valuable guidance for the maintenance, reliable operation and optimal design of MEMS applications. It can be concluded that different quality factors and residual stresses at various temperatures and vacuum levels have a significant effect on the vibration characteristics.

With prolonged vibration, significant cracking occurs on the surface of microbeams, which could affect the static deflection and the natural frequency of the structure. In 2020, K. Larkin et al. [22] investigated the nonlinear vibration response of a cracked MEMS gyroscope using the Griffith strain energy release theorem. This numerical study demonstrates that the presence of a severe single crack or a series of cracks could considerably affect the sensitivity of the gyroscope, resulting in degradation of the performance of the damaged MEMS sensor. In the following year, K. Larkin's team analyzed the effect of cumulative damage on the performance of electrically driven cantilever micro-beams based on an effective modulus structure model, deriving the equations of motion and analyzing the reduced order model for actuators with surface cracks [23]. A fatigue damage model was proposed by Jiaxing Cheng et al. to quantify the damage caused by micro- and nano-cracks in crystalline silicon structures and native oxide layers, which can assess the fatigue lifetime of MEMS structures [24]. The results indicate that the accumulation of fatigue damage occurs mainly near

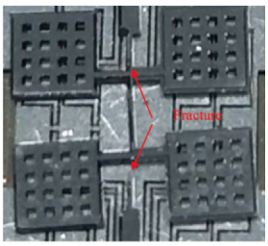

Fig. 1. Structure fracture of a MEMS gyroscope under random vibration [14].

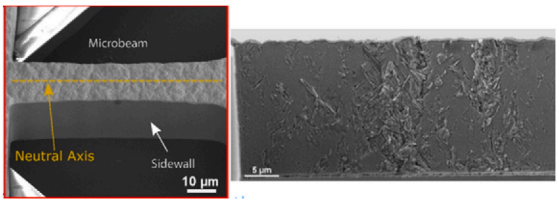

Fig. 2. Fatigue damage on a Ni microbeam [16].

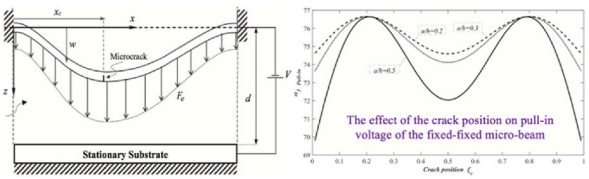

Fig. 3. Fatigue damage model of microbeam [17].

the root of the notch, which contributes to the cracks growth and the reduction in the resonant frequency.

In a word, the vibration-induced failures are mainly related to the resonant effect, material fatigue and micro-cracks propagation.

1.4. Vibration test methods

Vibration testing is used to reveal potential failure modes in MEMS device structures, metal leads and interconnects, and to assess device reliability. The commonly used vibration test methods are sinusoidal sweep and random vibration testing [25].

So far, although there is no international vibration test standard explicitly for MEMS inertial devices, there have been numerous studies suggesting various vibration test methods for different vibration environments. For example, D. Capriglione et al. [26] proposed a vibration test to detect mechanical stress effects on reliability and metrology performance in practical applications in MEMS testing and characterization. Han Woong Yoo et al. [27] developed a vibration test platform to accurately evaluate the reliability of MEMS resonators with external vibration coupling.

Several researchers have devised vibration test methods that can be applied to MEMS inertial devices by referencing international standards within MEMS-related fields. For instance, Domenico Capriglione et al. created a test rig utilizing sinusoidal sweep for automotive applications, referring to various international standards such as IEC 60068-2-6 (2009), AEC-Q100 rev. H (2014) and JESD22 B103B.01 (2016). Continuous sinusoidal sweep tests were performed in the frequency range of 20–2000 Hz, with the vibration acceleration of 2 g, 4 g or 8 g. Yao Liu et al. [14] carried out step tests on MEMS gyroscopes exposed to random vibration with root mean square accelerations of 3 g, 6 g, 25 g, 30 g, 35 g, 45 g, 50 g, 55 g, 60 g, and 62.5 g.

1.5. Design for vibration reliability

In terms of structural design, the reliability design of gold wire leads in MEMS inertial devices is essential to improving vibration reliability. The displacement and acceleration of gold wire leads under external acceleration were derived using the lead vibration equation [18]. The maximum positive stress σ_{wire_max} of the lead can be described as (1).

$$\sigma_{wire\_\max} \approx \frac{\rho L^2 Q_i a_0}{d} \tag{1}$$

where Q_i is the quality factor, L, d and ρ are the length, diameter and density of gold wire lead, respectively. a_0 is the amplitude of vibration acceleration. It was concluded that increasing lead diameter and shortening lead length would result in higher first-order natural frequency, preventing resonance and fracture failure, and improving lead reliability during vibration [18].

To prevent the performance instability of MEMS gyroscopes in random vibration environments, a combination of a long short-term memory (LSTM) network and a Kalman filter (KF) was proposed for error compensation by Chenhao Zhu [28]. Among them, the parameters of the Kalman filter were optimized iteratively using the Kalman smoother and expectation maximization (EM) algorithm. It was found that the combination method of bidirectional LSTM (BiLSTM), EM and KF results in a reduction of 46.54% and 22.30% in the standard deviation of the output signal (angular velocity) for the x-axis and z-axis, respectively.

In summary, in the domain of vibration reliability design, researchers primarily address issues of fatigue and fracture failure through structural design and theoretical modeling. In addition, errors caused by vibration are compensated based on artificial intelligence algorithms to avoid performance degradation. With the rapid development of artificial intelligence, error compensation algorithms based on AI for MEMS inertial devices will gain more attention of researchers.

2. MEMS reliability with consideration of shock

External shocks typically have large acceleration amplitudes, which largely impact the reliability of MEMS. The shock waveform is similar to a half-sine or square wave pulse. MEMS devices are subjected to unexpected or overloaded mechanical shock from time to time during normal operation. For instance, a large shock may be induced by a cell phone falling from a certain height, a car subjected to an external shock, a flying vehicle landing, or a cannonball launch [29,30]. Some typical shock scenarios are listed in Table 2 [31].

2.1. Typical shock failure modes

Shock stress is generated by external acceleration with a high amplitude and short pulse. The main failure modes of MEMS inertial devices under high-impact conditions include structural fracture, particle contamination, short circuit, adhesion, and delamination [32–34].

The fracture failure of comb and beam structures is a frequently occurring failure mode in MEMS inertial devices. When the impact stress exceeds the yield strength of the silicon material, the material cannot recover its original state due to plastic deformation, and fracture failure is likely to occur. Bing Bai et al. [35] applied a half-sine impact of 1500 g with a duration of 2 ms to a tuning fork gyroscope in six different impact directions, and the micro-beam root of the gyroscope fractured, as illustrated in Fig. 4.

During the fabrication of MEMS silicon structures, manufacturing processes such as deposition, etching, cutting, and assembly are prone to generate particulate defects and microcracks on the silicon wafer surface. For instance, particulate contamination is shown in Fig. 5 [36]. This phenomenon is exacerbated by external mechanical impacts, that is, the silicon residue particles can be transferred to anywhere in the cavity, resulting in the block of comb movement. Meanwhile, when the particles come into contact with other components, it can lead to short circuit failure.

For MEMS structures, the specific surface area (i.e. area divided by volume) is relatively large. In general, MEMS gyroscopes range in size from 1 to 100 μm, with tiny gaps (<1 μm) for capacitive combs. Therefore, its surface forces, including electrostatic force, capillary effect, and surface tension, play a dominant role. When MEMS devices are operated in severe shock environments, the suspended beam is subjected to significant bending deformation. If the surface stress of the comb exceeds its elastic stress and the displacement and deformation are greater than the comb gap, the movable comb will adhere to the substrate, eventually leading to stiction failure or short circuit failure [37]. Stiction failure is shown in Fig. 6.

2.2. Shock failure mechanisms

Shock loads are characterized by high acceleration amplitudes and short durations. In particular, the shock acceleration pulse does not simultaneously affect the whole structure region but is transmitted as a form of the stress wave. Technically, the impact response of MEMS structures ought to be calculated based on the theory of stress wave analysis [38]. However, applying the above theories to MEMS structures under diverse impact loads would result in heightened numerical modeling and computational difficulties. As a result, it is extremely significant to identify an appropriate response model for MEMS structural under shock. In general, analytical modeling and numerical analysis are the primary methods to analyze failure mechanisms.

2.2.1. Analytical models for shock

The single degree of freedom (SDOF) system model is the commonly used analytical model that is applied to calculate the structural response to shock [39]. For example, an approximate shock response to a ring vibration gyroscope was estimated using a SDOF model by Zhengcheng Qin et al. Therefore, the shock excitation displacement $x(t)$ of the vibration ring is calculated from the Duchenne integral, as shown in equation (2) [40].

$$\begin{cases} \dfrac{A}{\omega_d}\displaystyle\int_0^t \sin(\omega_s\tau)e^{\xi\omega_t(t-\tau)}\sin(\omega_d(t-\tau))d\tau \\ \qquad\qquad 0 \le t \le t_0 \\ \dfrac{A}{\omega_d}\displaystyle\int_0^{t_0} \sin(\omega_s\tau)e^{\xi\omega_t(t-\tau)}\sin(\omega_d(t-\tau))d\tau \\ \qquad\qquad t > t_0 \end{cases} \tag{2}$$

Table 2
Shock loads under different operating scenarios [31].

Scenarios	Shock loads
Falling	500~3000 g, 50–200 Hz
Vehicles	0~100 g, 5–50 Hz
Earthquake	0.1–0.5 g, 2–90 Hz
Shot	10^3~10^4 g,10^2~10^3 Hz
Hard Penetration	10^4~10^5 g,10^3~10^4 Hz
Spacecraft	10^3~10^4 g, 10^2~10^3 Hz
Artillery launch	10^4~10^5 g, 10^3~10^4 Hz

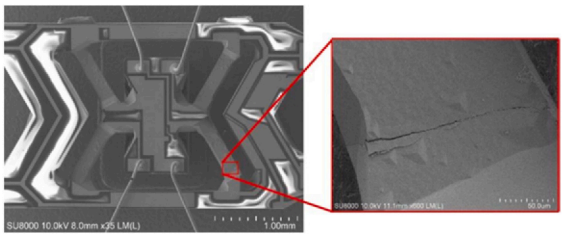

Fig. 4. Fracture failure of V-beam after the impact [35].

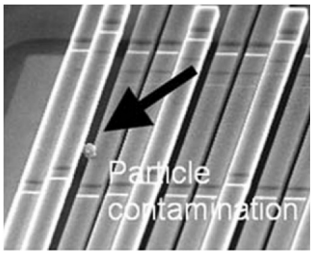

Fig. 5. Microparticle contamination [36].

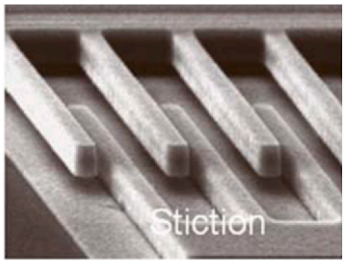

Fig. 6. Stiction failure caused by impact [36].

where ω_d and ω_s are the intrinsic angular frequencies of the drive mode and sense mode, respectively. ω_t is the resonant frequency of the MEMS gyroscope. ξ is the corresponding damping ratio.

In paper [41], the SODF shock response model for the gyroscope is derived in detail The response displacement $z(t)$ is solved according to equations (3) and (4), and Matlab simulation analysis and experimental verification are performed.

$$z(t) = R(t)u(t) + R(t-t_0)u(t-t_0) \tag{3}$$

$$\begin{aligned} R(t) &= \frac{\omega_0 A_i}{\omega_i\sqrt{1-\xi_i^{\,2}}} e^{-\frac{\omega_i}{2Q_i}} \sin\left(\sqrt{1-\xi_i^{\,2}}\,\omega_i t + \theta_i\right) + A_i \sin(\omega_0 t - \varphi_i) \\ A_i &= \frac{a_0}{\sqrt{\omega^4 + 2\left(2\xi_i^{\,2}-1\right)\omega_i{}^2\omega_0{}^2 + \omega_i{}^4}} \\ \varphi_i &= tg^{-1}\frac{\omega_i\omega_0}{Q_i(\omega_i{}^2-\omega_0{}^2)}, \theta_i = tg^{-1}\frac{\sqrt{1-\xi_i^{\,2}}}{\xi_i^{\,2} - Q_i(\omega_i{}^2-\omega_0{}^2)/\omega_i{}^2} \end{aligned} \tag{4}$$

where, ω_i and ω_0 are the natural angular frequencies of the gyroscope and external shock acceleration, respectively. ξ_i is the damping ratio and Q_i is the quality factor of the gyroscope. a_0 is the amplitude of shock acceleration.

Owing to the large amplitude and short duration of the shock, the transient and steady-state responses of the structure must be considered simultaneously. Transient responses to high-g impacts tend to induce structural vibrations that decay with time [42]. Recently, an analytical model was reported by Tianfang Peng et al. to describe the transient response under high-g shock, considering the decay of amplitude and frequency. The accuracy of the model was confirmed through numerical analysis results based on Shock Response Spectra (SRS) [43]. A model for high-g shock response was proposed by Kaisi Xu et al. to rapidly estimate the response of MEMS structures using a transfer function [44].

Tingting Huang et al. investigated the degradation process of devices in dynamic environments and developed a shock degradation

model based on the effective shock function and the Wiener process [45]. Nevertheless, the above studies only investigate one type of shock and rarely consider multiple shock processes that are widely available in practical applications. To address this point, Hongda Gao et al. developed four different dependent competitive failure models for degraded systems with multiple random shocks and derived reliability indicators [46].

According to the aforementioned models, it is possible to obtain the impact response acceleration and calculate the maximum impact stress on the structure. The main failure mechanisms of weak parts fractured due to impact, such as capacitive combs or spring beams, include collision or impact stress exceeding the yield strength of silicon material and stress concentration.

To sum up, although significant advancements have been made in modeling the shock response of MEMS structures under impact conditions, due to the intricate microstructure, shock response, and absence of experimental verification for transient processes, the existing studies exist the following deficiencies: (1) The theoretical model has yet to be fully verified through experimentation. (2) There is a relative lack of studies on the effects of different types of damping and nonlinear factors on the microstructure under shock conditions. These shortcomings require further overcoming in the future.

2.2.2. *Shock finite element analysis*

The Finite Element Method (FEM) is the most widely used numerical method for calculating the impact response of microstructures, including the calculation of the natural frequency, the operating mode, and the stress distribution of MEMS devices under shock. For example, Jinkui Wang et al. calculated the first four orders of modalities of a MEMS gyroscope by FEM, as well as the stress distribution and maximum stress values in different directions under an impact amplitude of 20,000 g [47]. Failure modes of MEMS gyroscopes under typical shock during artillery firing were investigated using FEM by Jiangkai Lian. The analysis results demonstrated that the shock of continuous oscillatory acceleration had a significant amplification effect on the stresses in the gyroscope structure [48].

The conclusion from the impact test was that the FEM simulation results are consistent with those of the model analysis. The main failure mechanisms are that the impact stress is far greater than the yield strength of the material due to stress concentration, leading to fracture failure.

2.3. *Shock test methods*

MEMS shock experiments require high amplitude and short duration mechanical loads, which bring some challenges to the waveform control and real-time data acquisition techniques. The general impact test equipment mainly includes Machete Hammers and Hopkinson Bar [31]. The waveforms of the shock signals generated by Machete Hammers and Hopkinson Bar are similar to a half-sinusoidal wave. In terms of damage characterization methods, the most commonly used instruments are scanning electron microscopy (SEM) and X-ray energy spectrometry (EDS) [49]. Up to now, there are still some new shock test methods worth exploring and researching.

Since there is no unified test method or standard for MEMS devices, researchers mainly refer to national or international standards for impact testing. To compare the reliability of different MEMS accelerometers in space applications, I. Marozau et al. applied shock accelerations of 5000 g and pulse duration of 2 ms to a variety of test devices [8]. To validate the theoretical analysis results, Yiyuan Li et al. exerted a shock to the MEMS-suspended inductors with amplitudes ranging from 8500 to 20400 g and durations ranging from 100 to 120 μs impact pulses by using a Machete Hammer [32]. MEMS gyroscope impact tests were conducted by Jiangkai Lian, with an acceleration of 15,000 g and duration of 100 μs, to simulate the high-g shock caused by shell launch. It was found that the critical

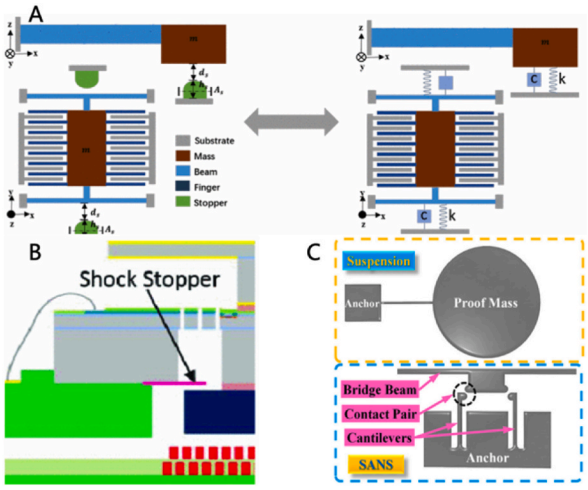

Fig. 7. Nonlinear spring model of the stopper; (B) Polymer three-dimensional impact baffle based on micro stereolithography; (C) Structure schematic of SANS.

acceleration for shock failure decreases with successive shocks of acceleration [48].

2.4. Design for shock reliability

Currently, the main shock-resistant design methods include optimizing the design of beam structures, adding buffer structures, adoption of energy dissipation, and using shock-resistant packaging technology. Tianfang Peng et al. optimized the shapes of MEMS cantilever beams, comb beams, island beams, and folded beams. The research results showed that various shock resistance properties of MEMS inertial devices were improved by 13–79% [50]. For buffer structures, it reduces impact stress as well as protects the MEMS structure. Tianfang Peng's team optimized the parameters of MEMS anti-overload structure by FEM, which effectively improved the anti-overload capability of MEMS stopper [51]. Sébastien Lani et al. designed a polymer three-dimensional (3D) impact baffle based on micro stereolithography, which increases impact resistance by four times and withstands an impact of up to 1000 g [52]. In addition, an adaptive nonlinear stopper (SANS) was proposed by Kaisi Xu et al. that can reduce the impact force by about 89.4% [53]. The SANS has three shock protection modes that are determined by the shock's magnitude, allowing for self-adaptive capability. The above-mentioned structures that provide shock resistance can be seen in Fig. 7.

Although the stoppers mitigate the effect of shocks, they increase the non-linearity of the system, which reduces the accuracy and sensitivity of detection. Consequently, to achieve a balance between impact resistance and mechanical sensitivity, Yang Gao increased the resonant frequency of the MEMS gyroscope and adopted a two-stage elastic baffle structure. The shock tests indicated that the proposed structure could withstand impacts of up to 10,000 g [54]. However, the baffle structures could potentially lead to particle contamination and short circuits due to silicon residues generated during impact. Thus, it is necessary to employ support structures to prevent mechanical collisions between structures, isolate the transfer of stresses, and reduce impact stresses.

With respect to energy dissipation, several researchers have proposed various materials with low coefficients of restoration (COR) as contact materials, namely, shock absorbers. Three-dimensional (3D) nanoscale lattices have attracted significant attention as structural materials for mechanical energy dissipation due to their excellent mechanical elasticity and high damping capacity [55]. A vertically aligned 3D nanocomposite based on ceramic-reinforced carbon nanotube (CNT) arrays was proposed by Eunhwan Jo et al. for in-plane damping and energy dissipation materials for MEMS with in-plane shock reliability over a wide acceleration range (0–12, 000 g) [56]. In the impact drop test, samples with nanotube arrays had approximately 115% and 80% higher survival rates (average acceleration at rupture of 10,000 g) compared to controls (no nanotubes) with hard-stop and flexible spring dampers, respectively.

In terms of shock-resistant packaging technology, Yunbo Shi et al. designed an efficient packaging method based on a three-layer wafer-level silicon chip [19], as shown in Fig. 8. The packaging method ensured that the measurement accuracy of the sensor under an impact of 200,000 g was better than 5%. This method starts by bonding the chip to the package shell, effectively insulating it from stress waves by controlling the parameters of the patch rubber, and then filling it with potting glue to increase the equivalent stiffness and achieve high natural frequency and unloading efficiency. The term "high solid" refers to the high natural frequency of the packaging body, and "wave unloading" refers to the ability to filter mechanical stress waves.

In regard to system-level structure design, Mohammad Fathalilou et al. proposed a dual-mass MEMS shock sensor (switch) that improve the safety performance of the sensor under below-threshold shocks by adjusting the auxiliary system, namely by attaching an auxiliary mass-spring to the main structure [57]. Danmeng Wang devised a Trap-and-Hold (TAH) additional structure to effectively restrict the motion of the mass when subjected to a shock, thereby enhancing the shock resistance of the dual-mass gyroscope [58]. The summary of the shock reliability design for the past five years is summarized in Table 3.

3. MEMS reliability with consideration of temperature

3.1. Typical thermal failure modes

Due to the widespread use of MEMS devices, they are inevitably exposed to high temperatures of 85 °C or even 125 °C. Temperature also has a significant influence on MEMS reliability. At high temperatures, thermal stresses generated by different materials can cause deformation of the sensor package, which can lead to bias and scale factor instability. The failure modes mainly include fatigue, fracture, open circuit, and delamination [62,63].

Fatigue originates from subcritical cracking caused by material surface roughness, while temperature increase intensify the material creep and accelerate crack growth until fracture failure occurs. The long-term thermal stress will lead to microcracks in the MEMS device solder joints. With the propagation of microcracks, the solder joints will eventually fall off, resulting in open-circuit

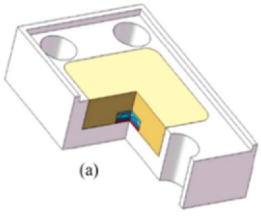

Fig. 8. Diagram of the "High solid-unloading wave" packaging technology [19].

Table 3
Summary of the shock reliability design in the past five years.

Devices	The design for shock reliability	Performance of MEMS devices	Year	Ref.
MEMS actuators	The optimal shape of MEMS beam (cantilever-mass, beam-comb, beam-island and folded beam)	Improvements of 13–79 % in different performance objectives	2022	[50]
MEMS gyroscopes	A vertically aligned 3D nanocomposite based on ceramic-reinforced carbon nanotube (CNT) arrays for shock absorbers of gyroscopes	The in-plane shock reliability is over a wide acceleration range (0–12,000 g).	2023	[56]
	Optimizing the design of MEMS stopper's shape and stiffness	The maximum stress of the beam-mass structure was decreased by 70 %	2021	[51]
	A structure of Trap-and-Hold (TAH) to effectively restrict the movement of the mass	The after-shock Angle Random Walk (ARW) was 0.0483 deg/rt-hr and the in-run bias instability (IrBS) was 0.69 deg/hr.	2020	[58]
	Epitaxially encapsulated (EPI) MEMS disc resonating gyroscopes (DRGs)	Maximum 50,000g impact with structural integrity and nearly constant resonance frequency (1.34 ppm change)	2020	[59]
	Optimizing the thickness of V-shaped beam of quartz tuning forks resonant gyroscope	Optimized beam thickness of 80 μm with a maximum stress of 94.721 MPa, which is able to tolerate an shock with an amplitude of 1500 g and a duration of 2 ms.	2020	[35]
	Enhancing the equivalent stiffness of the tuning fork gyroscope by restraining the movement of the quality mass	Improvement of impact resistance until failure at peak acceleration of 20,000 g and duration of 80 μs.	2019	[60]
MEMS switch	A MEMS bidirectional inertial switch with multiple acceleration thresholds	The acceleration thresholds are 69 g and 121 g, respectively, with tuning capability for greater robustness.	2022	[61]
	A MEMS dual-mass shock sensor with higher reliability	The interval between the designed threshold and the minimum shock has been decreased up to 45%.	2020	[57]

failure.

Generally, MEMS devices are manufactured by anodic bonding, which means that silicon and glass are bonded together. The anodic bonding process is achieved by applying an electrical potential difference between the two ends at a specific temperature [64]. For silicon-glass bonding, shear stress occurs at the interface between the two materials under high temperatures or temperature cycling due to their different coefficients of thermal expansion [65]. Although the thermal stress is significantly lower than the bonding strength of silica-glass, its prolonged exposure may promote the formation and expansion of microcracks, eventually leading to delamination failure. The accelerometer sensor illustrated in Fig. 9 possesses a significant area aspect ratio and triggers delamination as a result of high thermomechanical stresses during the soldering process [2].

3.2. Thermal failure mechanisms

3.2.1. Analytical models for thermal

Jacek Nazdrowicz et al. investigated the thermal expansion phenomenon of MEMS devices and its effect on various performance parameters [66]. Theoretical calculations and simulations showed that the quality factor and the natural frequency were most affected by ambient temperature. The quality factor was gradually degraded at high temperatures, and the non-linear variation of the natural frequency with temperature led to drifting of the MEMS parameters and unstable performance [67]. In addition, the effects of temperature on differential capacitance and output voltage were investigated by Jacek Nazdrowicz [68]. The zero bias of the vibratory gyroscope changes with ambient temperature due to thermal mismatch and degradation of the quality factor, eventually leading to instability in gyroscope performance. In brief, the thermal failure mechanisms mainly comprise the thermal mismatch, the temperature drift of the natural frequency and degradation of the quality factor.

3.2.2. Thermal finite element analysis

Due to the complex structure of MEMS sensors, different material properties, and large dimensional errors, it is challenging to develop accurate theoretical models based on temperature effects. Thus, Huichao Shi et al. used the finite element method (FEM) to model the temperature effects for electrothermally excited MEMS resonant sensors and study the effects of ambient temperature and inherent temperature rise on the MEMS structure [69]. The conclusions showed that the resonant frequency slightly changed with the increase in static excitation power. The effect of the inherent thermal temperature rise on the resonant frequency proved negligible, and the frequency shift caused by inherent thermal temperature remained constant. The resonant frequency decreased gradually with the increase in ambient temperature, and the frequency shift introduced by the ambient temperature was significantly greater than that caused by the inherent thermal temperature rise. Jacek Nazdrowicz et al. performed a simulation analysis of a MEMS accelerometer, which operated within the temperature range of 293.15–393.15 K [70]. Assuming that the device was an elastic solid object and that the inertial acceleration and ambient temperature were applied uniformly to the device, a modal analysis based on thermal-mechanical-electrostatic coupling was performed. A static study of the device was conducted to evaluate the displacement and extension of particular parts of the accelerometer. It was concluded that the thermal expansion shifted the electrodes, causing unnecessary capacitance and measurement signal errors, and that larger shifts also damaged the MEMS devices, resulting in structural failure.

3.3. Testing methods under thermal loads

According to literature research [71,72], there are two general categories of test methods under thermal loads: the temperature step test and the temperature cycling test.

For the temperature step test, Marcantonio Catelani et al. designed a temperature step test for sensors employed in aerial inertial measurements [73], which included the following steps: (1). The temperature was lowered to −20 °C after 15 min of exposure at −20 °C. (2). The temperature was raised by 5 °C at the fastest possible rate, followed by 15 min of exposure at the temperature reached, and then repeated until the temperature reached 60 °C.

For the commercial automotive industry, Maxime Auchlin et al. developed a temperature cycling test method methodology based

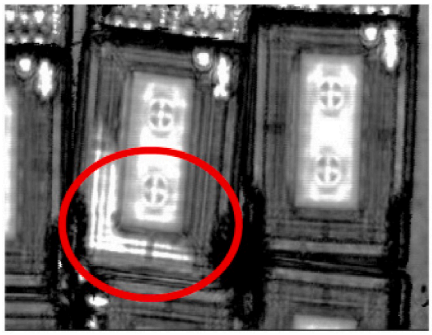

Fig. 9. Delamination failure induced by thermal stress [2].

Table 4
Summary of the temperature reliability design in the past six years.

Devices	The design for thermal reliability	Performances of MEMS devices	Year	Ref.
MEMS gyroscopes	Temperature compensation models of first-order, second-order, and higher-order based on the particle swarm optimization algorithm	The SD (standard deviation) of the output signal was reduced by about four times.	2021	[83]
	Bias drift compensation algorithm for the MEMS gyroscope with atmosphere package	A total bias error of 0.01 °/s over a temperature range of 7~45 °C	2020	[63]
	Back propagation artificial neural networks for temperature calibration	The accuracy of MEMS gyroscopes was improved by 20 %.	2018	[78]
	The quality factor of the bifurcation sensor was increased to 1000	Mechanical-thermal and electrical-thermal noise have no influence on the bifurcation sensors.	2021	[84]
	Enhancing the thermal stability of quality factor based on Joule effect in situ dynamic tuning by unitizing an active control loop	Zero bias thermal drift improved by more than three times in the 100 °C range	2023	[85]
MEMS accelerometer	Temperature drift compensation algorithm based on deep long short-term memory (DLSTM) and improved sparrow search algorithm (ISSA)	the three Allen variance coefficients of the MEMS accelerometer that bias instability, rate random walk, and rate ramp are improved from 5.43×10^{-4} mg,4.33×10^{-5} mg/s$^{1/2}$, 1.18×10^{-6} mg/s to 2.77×10^{-5} mg, 1.14×10^{-6} mg/s$^{1/2}$, 2.63×10^{-8} mg/s, respectively.	2023	[86]
	A reliable dual axis capacitive MEMS accelerometer	Detecting the acceleration in the range of ± 50 g with a capacitance sensitivity of 38 fF/g in the temperature range of -40 °C to 100 °C	2020	[81]

on the standard MIL-STD-883 K (method 1010). This test method involves cycling at −40 to 110 °C, with a heating or cooling rate of 2 °C/min and a rest time of 10 min [74]. Domenico Capriglione et al. proposed an Environmental Stress Screening (ESS) test procedure based on thermal cycling and mechanical vibration [75], in which the thermal cycling test was designed with reference to three standards, namely IEC 60068-2-14, MIL-STD 810G, and JEDEC JESD22 A104E. The test consists of four repetitive steps: (1). 1 h at low-temperature T_A; (2). The temperature rises at a certain rate from T_A to T_B; (3). 1 h at high-temperature T_B; (4). The temperature drops at a certain rate from T_B to T_A.

3.4. Design for thermal reliability

According to the previous analysis, it is evident that the performance of MEMS devices is affected by ambient temperature alterations. Achieving high vacuum packaging is a critical factor in solving this problem. MM Torunbalci et al. proposed a novel and simple method for all-silicon wafer-level fabrication and hermetic packaging of MEMS devices. The package remained hermetically sealed after temperature cycling (25°C–85 °C) and severe temperature shock (5 min at 300 °C) testing. And the bias instability and temperature sensitivity were 2.3 times and 4 times higher, respectively, compared to the MEMS sensors fabricated using silicon-on-glass (SOG) technology [76]. To solve the thermal stress mismatch, a novel 3D sandwich packaging technique consisting of composite substrate-Silicon-On-Insulator(SOI)-glass cap was presented by Lu Jia to achieve ultra-high quality factor for MEMS vibrating gyroscopes [77].

In addition, the errors caused by temperature were compensated using AI algorithms and circuit design. For the compensation algorithm, Rita Fontanella et al. proposed a temperature compensation method with improved polynomial fitting using Back Propagation (BP) Neural Network for mapping thermal deviation variations [78]. Qi Cai et al. developed a parallel processing model based on a variational modal decomposition time-frequency peak filter and Beetle antennae search algorithm-Elman neural network (BAS-Elman NN) to compensate the drift of noise and zero bias [79]. To improve the bias stability, bandwidth, temperature drift coefficient, and nonlinearity of scale factor, For aspects of circuit design, Huiliang Cao et al. proposed a closed-loop control approach for the sense mode of a dual-mass MEMS gyroscope based on a bipolar temperature compensation method [80]. A pattern-matching MEMS gyroscope interface specialised integrated circuit (ASIC) with on-chip temperature compensation was reported by Huan Zhang et al. The experimental results show that the standard deviation of the scale factor was reduced to 11.2 % of the pre-compensation value and the standard deviation of the zero-bias was reduced to 2.5 % in the temperature range from −40 to 60 °C. The zero-bias instability of the gyroscope was reduced to 1.9°/h from 4.6°/h before compensation.

In terms of structural design, Tahir et al. designed a reliable dual-axis capacitive MEMS accelerometer with a capacitance sensitivity of 38 fF/g. Its operating temperature range was −40∼100 °C, and measurement range was −50∼50 g [81]. Cheng Tu et al. proposed a high-sensitivity temperature sensor with a double-ended and triple-ended tuning fork (D/TETF) coupling beam structure, whose measurement sensitivity was better than −1000 ppm/°C in the temperature range of 25∼60 °C [82]. A stress isolation frame that is co-faced with a sensitive structural layer was proposed by Jing Zhang et al. for thermal stress isolation of accelerometers. It has been shown that the stress isolation frame effectively reduces temperature sensitivity by one to two orders of magnitude at temperatures from −40 °C to 85 °C. Some of the thermal reliability design methods used in the past six years are summarized in Table 4.

3.5. MEMS reliability with consideration of multiphysics field coupling

For a long time, most researchers took only one environmental factor into account when analyzing the reliability of MEMS inertial devices. However, it is not enough since the real application scenarios are complex. That is, the external stresses induced by ambient temperature, vibration, and shock may exist at the same time. Complex interactions exist for Multiphysics field coupling, which makes the reliability of MEMS inertial devices difficult to evaluate [87,88]. Therefore, research on the failure modes and failure mechanisms of multi-physics field coupling and reliability assessment is an important direction to accelerate the development of MEMS applications.

3.6. Electro-thermal-mechanical coupling

Electro-thermal-mechanical coupling behavior depends on temperature-dependent material parameters such as heat conductivity and coefficient of thermal expansion (CTE). The heat conductivity and CTE vary with temperature, which in turn affects Joule heating and heat conduction, causing different degrees of deformation in the beam structure. Under long-term operating conditions, the structure undergoes fatigue or creep, resulting in cumulative thermal-mechanical coupling damage [89].

Therefore, in order to comprehend how high temperatures affect MEMS properties, it is necessary to carry out a theoretical analysis of thermomechanical multi-physical field coupling [90].

In 2021, Liaxing Cheng et al. established a creep damage model based on continuous damage mechanics and performed a long-term performance analysis of MEMS actuators with thermomechanically coupled damage behavior [91]. The proposed continuum damage mechanics (CDM) model could be used to evaluate the effects of irreversible damage (cracks and deformations) on structural reliability under thermomechanical coupling as well as to conduct lifetime prediction analysis. Besides, an electro-thermal-mechanical model was proposed by Linfeng Zhao to analyze the temperature distribution and mechanical parameters of V-shaped actuators and complex drive structures [90]. The proposed coupling model could accurately calculates the temperature distribution and displacement of the V-beam, and precisely predict the behavior of the driving structure of the V-shaped actuator.

3.7. Thermal-shock coupling

Previous studies only considered single thermal or mechanical stresses on MEMS sensors without accounting for their environmental adaptability under complex stresses. However, MEMS often face both thermal and mechanical stresses in real-world applications. In high-temperature or temperature-cycling environments, the effects of mechanical vibration stresses are amplified, accelerating the development of reliability issues in MEMS devices.

Under thermal stress, high-risk connections are frequently subjected to significant levels of stress. Fatigue cracks develop in the joints between the solder and the pad. Similarly, the maximum stress occurs in the same areas during mechanical shock loads. With the thermal-shock coupling, the maximum stress at the connections will keep rising. Shuye Zhang et al. used COMSOL Multiphysics to analyze the mechanical performance of MEMS devices subjected to the coupled load of thermal cycling from −55 °C to 125 °C and 1500 g, 1 ms half-sine pulse shock [92]. Thermal stress and shock stress tend to cause stress concentration at the same position of the structure, enhancing the damage. Failure may occur if the combined stress exceeds the fracture strength. However, no further experimental validation was performed in this study.

To study the overall failure process of the device, a competing failure model based on extreme impact damage and a δ-impact competing failure model considering strong impacts were proposed by X. Wang [93]. The term "competitive failure" describes both the hard failures that result from external random shocks and the soft failures caused by the gradual degradation process that is affected by ambient temperature. These failures are interdependent [94]. Each unforeseen disturbance results in an additional abrupt escalation in the system's degradation, while the overall degradation lowers the threshold for hard failure [95].

So far, few studies on the reliability simulation of MEMS inertial devices under multiphysics field coupling environments have been reported, as well as the theoretical models and experimental tests.

3.8. Thermal-vibration coupling

The research on the coupling of temperature and vibration in MEMS has mainly focused on the silicon through-hole (TSV) structure of the devices. In 2019, Zhengwei Fan et al. studied the reliability of a typical TSV structure under thermal-vibration coupled loading, and obtained the maximum equivalent force, elastic and plastic strain response of the structure [96]. In 2020, based on fatigue theory and the multi-field coupling principle, Zhengwei Fan proposed a numerical analysis method for through-silicon-via copper (TSV-Cu) and analyzed the fatigue lifetime of the MEMS structure under thermal-vibration [97]. It was concluded that the fatigue lifetime was affected by the thermal-vibration stress obviously. However, there is a lack of detailed research on the reliability of MEMS inertial devices under multi-physical field coupling of thermal cycling and vibration. Similarly, there are few reports about the corresponding simulation, modeling, and experimental tests.

4. Conclusion

This paper reviews the main failure modes, failure mechanisms, test methods and reliability design of MEMS inertial devices under vibration, shock, thermal and coupling stress in the last five to six years. It can provide a guidance for the future failure analysis and reliability design of MEMS inertial devices. The conclusions are drawn as follows: (1) Although the research models for different environmental stresses are various, most of the studies contain three main parts: theoretical modelling, finite element simulation, and experimental validation; (2) Through a large number of literature studies, it is found that there are many and relatively complete reliability studies on MEMS inertial devices under single environmental stress at present, but there are few reliability studies on MEMS inertial devices under composite stress, lacking systematic research. (3) The main challenges for the reliability study under composite stress environment are as follows: i) It remains a challenge to develop a theoretical model of the failure mechanism; ii) Lack of professional coupling stress testing equipment; iii) Lack of corresponding test standards and evaluation methods.

Although MEMS inertial devices have been widely used in recent years, and their performance and function test standards are relatively complete, there is a lack of corresponding reliability test standards. At present, the reliability test of MEMS inertial devices mainly refers to the reliability test standards of integrated circuits and electronic components, such as MIL-STD-810G, MIL-STD-883H, JESD22 B103B, IEC 60068, and AEC-Q100. Hence, future research should focus on the following directions:

1). Multiphysical field coupling simulation: It is necessary to develop more accurate and reliable simulation methods for multi-physical field coupling to further reveal the critical factors affecting the reliability of MEMS inertial devices.
2). Novel theoretical modelling approaches: Based on the existing theoretical models, the complexity of the materials and structures in the devices is considered to better predict and assess the reliability of MEMS inertial devices.
3). Design of composite stress tests: more complex composite stress tests should be designed and carried out to more realistically simulate the stress conditions in the working environment and to investigate their impact on the reliability of MEMS inertial devices.
4). Developing specific test standards: The research on the reliability of MEMS inertial devices requires specific test and evaluation methods to better assess the reliability performance in complex operating environments and to provide a more accurate and reliable reference basis for reliability design in practical applications.

Data availability statement

The authors do not have permission to share data.

CRediT authorship contribution statement

Yingyu Xu: Investigation, Writing – original draft. **Shuibin Liu:** Data curation, Investigation. **Chunhua He:** Methodology, Writing – original draft. **Heng Wu:** Writing – review & editing. **Lianglun Cheng:** Project administration. **Guizhen Yan:** Resources, Supervision. **Qinwen Huang:** Formal analysis, Funding acquisition.

Declaration of competing interest

The authors declare that they have no known competing financial interests or personal relationships that could have appeared to influence the work reported in this paper.

Acknowledgements

This work was partially supported by the National Natural Science Foundation of China (Grant Nos. 62104047, U22A2012 and 62173098), Guangdong Basic and Applied Basic Research Foundation (Grant No. 2023A1515010291), and Basic and Applied Basic Research Foundation of Guangzhou Basic Research Program (Grant No. 2023A04J1707).

References

[1] M.I. Younis, MEMS Linear and Nonlinear Statics and Dynamics, Springer Science & Business Media, 2011.
[2] M. Hommel, H. Knab, S.G. Yousef, Reliability of automotive and consumer MEMS sensors-An overview, Microelectron. Reliab. 126 (2021) 114252, https://doi.org/10.1016/j.microrel.2021.114252.
[3] A.S. Algamili, M.H.M. Khir, J.O. Dennis, A.Y. Ahmed, S.S. Alabsi, S.S. Ba Hashwan, M.M. Junaid, A review of actuation and sensing mechanisms in MEMS-based sensor devices, Nanoscale Res. Lett. 16 (2021) 1–21, https://doi.org/10.1186/s11671-021-03481-7.
[4] M.K. Mishra, V. Dubey, P.M. Mishra, I. Khan, MEMS technology: a review, J. Eng. Res. Rep. 4 (2019) 1–24.
[5] H. Sun, M. Yin, W. Wei, J. Li, H. Wang, X. Jin, MEMS based energy harvesting for the Internet of Things: a survey, Microsyst. Technol. 24 (2018) 2853–2869, https://doi.org/10.1007/s00542-018-3763-z.
[6] M.Y. Fan, L.F. Zhang, Research Progress of Quartz Tuning Fork Micromachined Gyroscope, Atlantis Press, 2015, pp. 361–364, https://doi.org/10.2991/aiie-15.2015.100.
[7] J. Iannacci, Reliability of MEMS: a perspective on failure mechanisms, improvement solutions and best practices at development level, Displays 37 (2015) 62–71, https://doi.org/10.1016/j.displa.2014.08.003.
[8] I. Marozau, M. Auchlin, V. Pejchal, F. Souchon, D. Vogel, M. Lahti, N. Saillen, O. Sereda, Reliability assessment and failure mode analysis of MEMS accelerometers for space applications, Microelectron. Reliab. 88 (2018) 846–854, https://doi.org/10.1016/j.microrel.2018.07.118.
[9] A.L. Hartzell, M.G. Da Silva, H.R. Shea, MEMS Reliability, Springer Science & Business Media, 2010.
[10] J. Zhu, X. Liu, Q. Shi, T. He, Z. Sun, X. Guo, W. Liu, O.B. Sulaiman, B. Dong, C. Lee, Development trends and perspectives of future sensors and MEMS/NEMS, Micromachines 11 (2019) 7, https://doi.org/10.3390/mi11010007.
[11] M. Varanis, A. Silva, A. Mereles, R. Pederiva, MEMS accelerometers for mechanical vibrations analysis: a comprehensive review with applications, J. Braz. Soc. Mech. Sci. Eng. 40 (2018) 1–18, https://doi.org/10.1007/s40430-018-1445-5.
[12] A. Somà, A survey of Mechanical failure and design for Reliability of MEMS, in: IOP Conference Series: Materials Science and Engineering, IOP Publishing, 2020 012051, https://doi.org/10.1088/1757-899X/724/1/012051.
[13] N. Labat, F. Marc, H. Frémont, N. Nolhier, in: Proceedings of the 32nd European Symposium on the Reliability of Electron Devices, Failure Physics and Analysis, Microelectronics Reliability, 2021 114403, https://doi.org/10.1016/j.microrel.2021.114403.
[14] Y. Liu, H. Ge, Z. Fan, X. Chen, F. Huang, Y. Wang, Z. Hou, G. Bai, Failure analysis and experimental validation of MEMS Gyro under random vibration condition, in: 2019 Prognostics and System Health Management Conference (PHM-Qingdao), IEEE, 2019, pp. 1–6.
[15] E. Kakandar, A. Barrios, J. Michler, X. Maeder, G.M. Castelluccio, A computational and experimental Comparison on the Nucleation of fatigue cracks in statistical volume elements, Int. J. Fatig. 137 (2020) 105633, https://doi.org/10.1016/j.ijfatigue.2020.105633.
[16] S. Zhang, J. Zhang, Fatigue-induced dynamic pull-in instability in electrically actuated microbeam resonators - ScienceDirect, Int. J. Mech. Sci. 195 (2021), https://doi.org/10.1016/j.ijmecsci.2020.106261.
[17] S.A. Tajalli, S.M. Tajalli, Wavelet based damage identification and dynamic pull-in instability analysis of electrostatically actuated coupled domain microsystems using generalized differential quadrature method, Mech. Syst. Signal Process. 133 (2019) 106256, https://doi.org/10.1016/j.ymssp.2019.106256.
[18] C.H. He, Q.C. Zhao, Z.C. Yang, D.C. Zhang, G.Z. Yan, Micromechanical gyroscope vibration failure mechanism and reliability design research, Journal of Transduction Technology (2019) 1–6.
[19] Y. Shi, X. Wen, Y. Zhao, R. Zhao, H. Cao, J. Liu, Investigation and experiment of high shock packaging technology for high-G MEMS accelerometer, IEEE Sensor. J. 20 (2020) 9029–9037, https://doi.org/10.1109/JSEN.2020.2987971.
[20] Y. Liu, S. Zhang, Z. Hou, Z. Fan, Y. Wang, X. Peng, X. Chen, An investigate on degradation models of resonant frequency and mechanical sensitivity for butterfly resonator gyroscope, J. Microelectromech. Syst. 29 (2020) 468–479, https://doi.org/10.1109/JMEMS.2019.2957495.
[21] W. Luo, W. Su, Z. Nie, Q. Huang, S. Li, X. Dong, Vibration characteristic measurement method of MEMS gyroscopes in vacuum, high and low temperature environment and verification of excitation method, IEEE Access 9 (2021) 129582–129593, https://doi.org/10.1109/ACCESS.2021.3111629.
[22] K. Larkin, M. Ghommem, A. Hunter, A. Abdelkefi, Nonlinear modeling and performance analysis of cracked beam microgyroscopes, Int. J. Mech. Sci. 188 (2020) 105965, https://doi.org/10.1016/j.ijmecsci.2020.105965.
[23] K. Larkin, A. Hunter, A. Abdelkefi, Comparative investigations of multi-fidelity modeling on performance of electrostatically-actuated cracked micro-beams, Int. J. Mech. Sci. 192 (2021) 106139, https://doi.org/10.1016/j.ijmecsci.2020.106139.
[24] J. Cheng, Z. Qian, Z. Li, A cumulative fatigue damage model of polysilicon films for MEMS resonator under repeated loadings, Int. J. Fatig. 147 (2021) 106186, https://doi.org/10.1016/j.ijfatigue.2021.106186.
[25] D. Capriglione, M. Carratù, M. Catelani, L. Ciani, G. Patrizi, A. Pietrosanto, R. Singuaroli, P. Sommella, Performance analysis of MEMS-based inertial measurement units in terrestrial vehicles, Measurement 186 (2021) 110237, https://doi.org/10.1016/j.measurement.2021.110237.

[26] D. Capriglione, M. Carratù, M. Catelani, L. Ciani, G. Patrizi, R. Singuaroli, A. Pietrosanto, P. Sommella, Development of a test plan and a testbed for performance analysis of MEMS-based IMUs under vibration conditions, Measurement 158 (2020) 107734, https://doi.org/10.1016/j.measurement.2020.107734.
[27] H.W. Yoo, R. Riegler, D. Brunner, S. Albert, T. Thurner, G. Schitter, Experimental evaluation of vibration influence on a resonant MEMS scanning system for automotive Lidars, IEEE Trans. Ind. Electron. 69 (2022) 3099–3108, https://doi.org/10.1109/TIE.2021.3065608.
[28] C. Zhu, S. Cai, Y. Yang, W. Xu, H. Shen, H. Chu, A combined method for MEMS gyroscope error compensation using a long short-term memory network and Kalman filter in random vibration environments, Sensors 21 (2021) 1181, https://doi.org/10.3390/s21041181.
[29] Z. Ni, Y. Liu, J. Xie, Y. Liao, J. Dai, Investigation on the design method and failure mechanism of silicon-based MEMS Setback Arming device, in: J. Tan (Ed.), Advances in Mechanical Design, Springer Nature, Singapore, 2022, pp. 2357–2374, https://doi.org/10.1007/978-981-16-7381-8_147.
[30] S. Vasagiri, R.K. Burra, J. Vankara, M.S.P. Kumar Patnaik, A survey of MEMS cantilever applications in determining volatile organic compounds, AIP Adv. 12 (2022) 030701, https://doi.org/10.1063/5.0075034.
[31] T. Peng, Z. You, Reliability of MEMS in shock environments: 2000-2020, Micromachines 12 (2021) 1275, https://doi.org/10.3390/mi12111275.
[32] Y. Li, J. Li, L. Xu, Failure mode analysis of MEMS suspended inductors under mechanical shock, Microelectron. Reliab. 85 (2018) 38–48, https://doi.org/10.1016/j.microrel.2018.03.041.
[33] M. Auchlin, New Reliability Assessment of MEMS Components under Accumulative Testing for Space Applications, EPFL, 2021, https://doi.org/10.5075/epfl-thesis-8670.
[34] S. Saraygord Afshari, F. Enayatollahi, X. Xu, X. Liang, Machine learning-based methods in structural reliability analysis: a review, Reliab. Eng. Syst. Saf. 219 (2022) 108223, https://doi.org/10.1016/j.ress.2021.108223.
[35] B. Bai, C. Li, Y. Zhao, Development of V-shaped beam on the shock resistance and driving frequency of micro Quartz tuning forks resonant gyroscope, Micromachines 11 (2020) 1012, https://doi.org/10.3390/mi11111012.
[36] L. Skogström, J. Li, T.T. Mattila, V. Vuorinen, Chapter 44 - MEMS reliability, in: M. Tilli, M. Paulasto-Krockel, M. Petzold, H. Theuss, T. Motooka, V. Lindroos (Eds.), Handbook of Silicon Based MEMS Materials and Technologies, third ed., Elsevier, 2020, pp. 851–876, https://doi.org/10.1016/B978-0-12-817786-0.00044-X.
[37] Y. Qiao, W. Xu, J. Sun, H. Zhang, Reliability of electrostatically actuated MEMS resonators to random mass disturbance, Mech. Syst. Signal Process. 121 (2019) 711–724, https://doi.org/10.1016/j.ymssp.2018.11.055.
[38] W.J. Stronge, Impact Mechanics, Impact Mechanics, by W. J. Stronge, Pp. 300. ISBN 0521602890, Cambridge University Press, Cambridge, UK, March 2004, https://doi.org/10.1017/CBO9780511626432, 100 (2004.
[39] V. Singh, V. Kumar, A. Saini, P.K. Khosla, S. Mishra, Response analysis of MEMS based high-g acceleration threshold switch under mechanical shock, Int. J. Mech. Mater. Des. 17 (2021) 137–151, https://doi.org/10.1007/s10999-020-09520-y.
[40] Z. Qin, Y. Gao, X. Ding, J. Jia, L. Huang, H. Li, Design and optimization of a vibrating ring gyroscope with high shock resistance by differential Evolution, IEEE Sensor. J. 21 (2021) 16510–16518, https://doi.org/10.1109/JSEN.2021.3077626.
[41] C.H. He, Micromechanical gyroscope impact characteristics and reliability study, Journal of Transduction Technology. 32 (20210430). http://chinatransducers.seu.edu.cn/ch/reader/view_abstract.aspx?file_no=274&flag=1 (accessed May 8, 2023).
[42] N.H. Chao, D.E. Carlucci, New electronic packaging method for potted guidance electronics to sustain temperature cycling and survive high-G applications, J. Electron. Packag. 141 (2019), https://doi.org/10.1115/1.4042471.
[43] T. Peng, Z. You, An analytical model of transient response of MEMS under high-G shock for reliability assessment, in: 2022 IEEE International Reliability Physics Symposium (IRPS), 2022, https://doi.org/10.1109/IRPS48227.2022.9764430. P41-1-P41-5.
[44] K. Xu, N. Zhu, F. Jiang, W. Zhang, Y. Hao, A transfer function approach to shock duration compensation for laboratory evaluation of ultra-high-G vacuum-packaged MEMS accelerometers, in: 2019 IEEE 32nd International Conference on Micro Electro Mechanical Systems (MEMS), 2019, pp. 676–679, https://doi.org/10.1109/MEMSYS.2019.8870797.
[45] T. Huang, B. Peng, D.W. Coit, Z. Yu, Degradation modeling and lifetime prediction considering effective shocks in a dynamic environment, IEEE Trans. Reliab. 68 (2019) 819–830, https://doi.org/10.1109/TR.2019.2917058.
[46] H. Gao, L. Cui, Q. Qiu, Reliability modeling for degradation-shock dependence systems with multiple species of shocks, Reliab. Eng. Syst. Saf. 185 (2019) 133–143, https://doi.org/10.1016/j.ress.2018.12.011.
[47] J. Wang, W. Lou, D. Wang, H. Feng, Design, analysis, and fabrication of silicon-based MEMS gyroscope for high-g shock platform, Microsyst. Technol. 25 (2019) 4577–4586, https://doi.org/10.1007/s00542-019-04596-9.
[48] J. Lian, Y. Li, Y. Tang, J. Li, L. Xu, Analysis of the vulnerability of MEMS tuning fork gyroscope during the gun launch, Microelectron. Reliab. 107 (2020) 113619, https://doi.org/10.1016/j.microrel.2020.113619.
[49] J. Qu, X. Liu, MEMS-based platforms for multi-physical characterization of nanomaterials: a review, IEEE Sensor. J. 22 (2022) 1827–1841, https://doi.org/10.1109/JSEN.2021.3135888.
[50] T. Peng, Z. You, The optimal shape of MEMS beam under high-G shock based on a probabilistic fracture model, in: 2022 IEEE International Reliability Physics Symposium (IRPS), 2022, https://doi.org/10.1109/IRPS48227.2022.9764507. P42-1-P42-5.
[51] T. Peng, Z. You, A computationally efficient model of MEMS stopper for reliability optimization, in: 2021 28th IEEE International Conference on Electronics, Circuits, and Systems (ICECS), 2021, pp. 1–6, https://doi.org/10.1109/ICECS53924.2021.9665627.
[52] S. Lani, O. Chandran, M. Auchlin, I. Marozau, B. Dunan, 3d printing on MEMS: integration of 3d shock stopper on a micro mirror, in: 2019 20th International Conference on Solid-State Sensors, Actuators and Microsystems & Eurosensors XXXIII (TRANSDUCERS & EUROSENSORS XXXIII), 2019, pp. 113–116, https://doi.org/10.1109/TRANSDUCERS.2019.8808274.
[53] K. Xu, F. Jiang, W. Zhang, Y. Hao, Micromachined integrated self-adaptive nonlinear stops for mechanical shock protection of MEMS, J. Micromech. Microeng. 28 (2018) 064006, https://doi.org/10.1088/1361-6439/aab581.
[54] Y. Gao, L. Huang, X. Ding, H. Li, Design and implementation of a dual-mass MEMS gyroscope with high shock resistance, Sensors 18 (2018) 1037, https://doi.org/10.3390/s18041037.
[55] E. Jo, H. Lee, J.-I. Lee, J. Kim, Mechanically resilient, alumina-reinforced carbon nanotube arrays for in-plane shock absorption in micromechanical devices, Microsyst Nanoeng 9 (2023) 1–9, https://doi.org/10.1038/s41378-023-00539-7.
[56] H. Lee, E. Jo, J.-I. Lee, J. Kim, MEMS shock absorbers integrated with Al2O3-reinforced, mechanically resilient nanotube arrays, in: 2023 IEEE 36th International Conference on Micro Electro Mechanical Systems (MEMS), 2023, pp. 45–48, https://doi.org/10.1109/MEMS49605.2023.10052484.
[57] M. Fathalilou, K. Soltani, G. Rezazadeh, E. Cigeroglu, Enhancement of the reliability of MEMS shock sensors by adopting a dual-mass model, Measurement 153 (2020) 107428, https://doi.org/10.1016/j.measurement.2019.107428.
[58] D. Wang, R.M. Noor, A.M. Shkel, Dynamically amplified dual-mass gyroscopes with in-situ shock survival mechanism, in: 2020 IEEE International Symposium on Inertial Sensors and Systems (INERTIAL), 2020, https://doi.org/10.1109/INERTIAL48129.2020.9090021, pp. 1–4.
[59] C.P. Cameron, T. Imamura, C. Devmalya, G. Vukasin, A. Alter, T. Kenny, Design comparison and survivability of epitaxially encapsulated MEMS disc resonating gyroscopes at high shock (>27,000g), in: 2020 IEEE International Symposium on Inertial Sensors and Systems (INERTIAL), 2020, https://doi.org/10.1109/INERTIAL48129.2020.9090024, pp. 1–4.
[60] J. Lian, J. Li, L. Xu, The effect of displacement constraints on the failure of MEMS tuning fork gyroscopes under shock impact, Micromachines 10 (2019) 343, https://doi.org/10.3390/mi10050343.
[61] A. Niyazi, Q. Xu, F. Khan, M.I. Younis, Design, modeling, and testing of a bidirectional multi-threshold MEMS inertial switch, Sensors and Actuators A: Physical. 334 (2022) 113219, https://doi.org/10.1016/j.sna.2021.113219.
[62] X. Wang, J. Yang, X. Liu, P. Zheng, Q. Song, B. Song, S. Liu, Reliability analysis of solder joints on rigid-flexible printed circuit board for MEMS pressure sensors under combined temperature cycle and vibration loads with continuously monitored electrical signals, J. Electron. Packag. 144 (2021), https://doi.org/10.1115/1.4049813.

[63] J. Liu, M. Fu, C. Meng, J. Li, K. Li, J. Hu, X. Chen, Consideration of thermo-vacuum stability of a MEMS gyroscope for space applications, Sensors 20 (2020) 7172, https://doi.org/10.3390/s20247172.

[64] R. Joyce, M. George, L. Bhanuprakash, D.K. Panwar, R.R. Bhatia, S. Varghese, J. Akhtar, Investigation on the effects of low-temperature anodic bonding and its reliability for MEMS packaging using destructive and non-destructive techniques, J. Mater. Sci. Mater. Electron. 29 (2018) 217–231, https://doi.org/10.1007/s10854-017-7908-0.

[65] F. Feng, P. Jia, J. Qian, Z. Hu, G. An, L. Qin, High-consistency optical fiber fabry-perot pressure sensor based on silicon MEMS technology for high temperature environment, Micromachines 12 (2021) 623, https://doi.org/10.3390/mi12060623.

[66] J. Nazdrowicz, A. Napieralski, Thermal expansion phenomena and influence on damping coeffcient and stiffness variation for MEMS kinematic quantity microsensors and microactuators, in: 2020 19th IEEE Intersociety Conference on Thermal and Thermomechanical Phenomena in Electronic Systems (ITherm), 2020, pp. 1246–1254, https://doi.org/10.1109/ITherm45881.2020.9190185.

[67] J. Nazdrowicz, A. Napieralski, Temperature change leverage on performance of MEMS rotational motion sensors, in: 2019 18th IEEE Intersociety Conference on Thermal and Thermomechanical Phenomena in Electronic Systems (ITherm), 2019, pp. 90–100, https://doi.org/10.1109/ITHERM.2019.8757355.

[68] J. Nazdrowicz, A. Napieralski, Analysis of temperature variation influence on capacitance inertial sensors parameters, in: 2020 19th IEEE Intersociety Conference on Thermal and Thermomechanical Phenomena in Electronic Systems (ITherm), 2020, pp. 1364–1373, https://doi.org/10.1109/ITherm45881.2020.9190506.

[69] H. Shi, G. Zhu, L. Cao, S. Fan, Study on temperature influence of an electrothermally excited MEMS resonant sensor based on finite element method, Microsyst. Technol. 27 (2021) 2705–2714, https://doi.org/10.1007/s00542-020-05060-9.

[70] J. Nazdrowicz, A. Napieralski, An analysis of temperature variation effect on response and performance of capacitive microaccelerometer inertial sensors, in: 2021 37th Semiconductor Thermal Measurement, Modeling & Management Symposium (SEMI-THERM), 2021, pp. 10–15.

[71] A. Thura, V.N. Goroshko, B.N. Simonov, S.P. Timoshenkov, Accelerated life time estimation of the MEMS devices in the thermal influence, in: 2018 IEEE Conference of Russian Young Researchers in Electrical and Electronic Engineering (EIConRus), 2018, pp. 1590–1594, https://doi.org/10.1109/EIConRus.2018.8317404.

[72] T.H. Papanchev, A.S. Georgiev, J.G. Garipova, A smart sensor modules reliability estimation by thermal cycling tests, in: 2019 IEEE XXVIII International Scientific Conference Electronics (ET), 2019, pp. 1–4, https://doi.org/10.1109/ET.2019.8878668.

[73] M. Catelani, L. Ciani, G. Patrizi, D. Capriglione, M. Carratù, P. Sommella, A. Pietrosanto, Design and experimental analysis of temperature tests for inertial measurement units in avionic applications, in: 2020 IEEE 7th International Workshop on Metrology for AeroSpace (MetroAeroSpace), 2020, pp. 217–221, https://doi.org/10.1109/MetroAeroSpace48742.2020.9160086.

[74] M. Auchlin, I. Marozau, D.Z. Bayat, L. Marchand, V. Gass, O. Sereda, Can automotive MEMS be reliably used in space applications? An assessment method under sequential bi-parameter testing, Microelectron. Reliab. 114 (2020) 113913, https://doi.org/10.1016/j.microrel.2020.113913.

[75] D. Capriglione, M. Carratù, A. Pietrosanto, P. Sommella, M. Catelani, L. Ciani, G. Patrizi, R. Singuaroli, L. Signorini, Characterization of inertial measurement units under environmental stress screening, in: 2020 IEEE International Instrumentation and Measurement Technology Conference (I2MTC), 2020, pp. 1–6, https://doi.org/10.1109/I2MTC43012.2020.9129263.

[76] M.M. Torunbalci, H.D. Gavcar, F. Yesil, S.E. Alper, T. Akin, An all-silicon process platform for wafer-level vacuum packaged MEMS devices, IEEE Sensor. J. 21 (2021) 13958–13964, https://doi.org/10.1109/JSEN.2021.3073928.

[77] L. Jia, G. Han, Z. Wei, C. Si, J. Ning, F. Yang, W. Han, A novel packaged ultra-high Q silicon MEMS butterfly vibratory gyroscope, Micromachines 13 (2022) 1967, https://doi.org/10.3390/mi13111967.

[78] R. Fontanella, D. Accardo, R.S. Lo Moriello, L. Angrisani, D. De Simone, MEMS gyros temperature calibration through artificial neural networks, Sensors and Actuators A: Physical. 279 (2018) 553–565, https://doi.org/10.1016/j.sna.2018.04.008.

[79] Q. Cai, F. Zhao, Q. Kang, Z. Luo, D. Hu, J. Liu, H. Cao, A novel parallel processing model for noise reduction and temperature compensation of MEMS gyroscope, Micromachines 12 (2021) 1285, https://doi.org/10.3390/mi12111285.

[80] H. Cao, Y. Liu, Y. Zhang, X. Shao, J. Gao, K. Huang, Y. Shi, J. Tang, C. Shen, J. Liu, Design and experiment of dual-mass MEMS gyroscope sense closed system based on bipole compensation method, IEEE Access 7 (2019) 49111–49124, https://doi.org/10.1109/ACCESS.2019.2909973.

[81] M.A.R. Tahir, S.A.R. Bukhari, M.M. Saleem, Reliability based design of MEMS accelerometer considering residual stress and temperature variations, in: 2020 IEEE 23rd International Multitopic Conference (INMIC), 2020, pp. 1–6, https://doi.org/10.1109/INMIC50486.2020.9318187.

[82] C. Tu, M. Yang, Z. Zhang, X. Lv, L. Li, X.-S. Zhang, Highly sensitive temperature sensor based on coupled-beam AlN-on-Si MEMS resonators operating in out-of-plane flexural vibration modes, Research 2022 (2022), https://doi.org/10.34133/2022/9865926, 2022/9865926.

[83] J. Wu, T. Huang, Z. Zhu, K. Song, Cold starting temperature time-related compensation model of inertial sensors based on particle swarm optimization algorithm, Rev. Sci. Instrum. 92 (2021) 065106, https://doi.org/10.1063/5.0050027.

[84] Y. Qiao, M. Arabi, W. Xu, H. Zhang, E.M. Abdel-Rahman, The impact of thermal-noise on bifurcation MEMS sensors, Mech. Syst. Signal Process. 161 (2021) 107941, https://doi.org/10.1016/j.ymssp.2021.107941.

[85] J. Cui, Q. Zhao, Thermal stabilization of quality factor for dual-axis MEMS gyroscope based on Joule effect in-situ dynamic tuning, IEEE Trans. Ind. Electron. (2023) 1–8, https://doi.org/10.1109/TIE.2023.3250739.

[86] G. Guo, B. Chai, R. Cheng, Y. Wang, Temperature drift compensation of a MEMS accelerometer based on DLSTM and ISSA, Sensors 23 (2023) 1809, https://doi.org/10.3390/s23041809.

[87] C. Comi, A. Corigliano, A. Frangi, V. Zega, Linear and nonlinear mechanics in MEMS, in: B. Vigna, P. Ferrari, F.F. Villa, E. Lasalandra, S. Zerbini (Eds.), Silicon Sensors and Actuators: the Feynman Roadmap, Springer International Publishing, Cham, 2022, pp. 389–437, https://doi.org/10.1007/978-3-030-80135-9_12.

[88] R.T. Raman, A. Ajoy, SPICE-based multiphysics model to analyze the dynamics of ferroelectric negative-capacitance-electrostatic MEMS hybrid actuators, IEEE Trans. Electron. Dev. 67 (2020) 5174–5181, https://doi.org/10.1109/TED.2020.3019991.

[89] L. Paoli, M. Shillor, A dynamic thermo-mechanical actuator system with contact and Barber's heat exchange boundary conditions, Proc. R. Soc. Edinb. Sect. A (Math. Phys. Sci.): Mathematics 151 (2021) 734–760, https://doi.org/10.1017/prm.2020.35.

[90] L.-F. Zhao, Z.-F. Zhou, M.-Z. Meng, M.-J. Li, Q.-A. Huang, An efficient electro-thermo-mechanical model for the analysis of V-shaped thermal actuator connected with driven structures, Int. J. Numer. Model. Electron. Network. Dev. Field. 34 (2021) e2843, https://doi.org/10.1002/jnm.2843.

[91] J. Cheng, Z. Li, Analysis of thermo-mechanical coupling damage behavior in long-term performance of microelectromechanical systems actuators, Int. J. Damage Mech. 31 (2022) 190–214, https://doi.org/10.1177/10567895211033972.

[92] S. Zhang, J. Xu, S. Zhang, P. He, M. Sun, J. Yang, X. Li, K.-W. Paik, Reliability analysis of 3D CSP MEMS and IC under thermal cycle-impact coupled multi-physics loads, in: 2021 IEEE 71st Electronic Components and Technology Conference (ECTC), 2021, pp. 1376–1381, https://doi.org/10.1109/ECTC32696.2021.00221.

[93] X. Wang, L. Li, M. Chang, K. Han, Reliability modeling for competing failure processes with shifting failure thresholds under severe product working conditions, Appl. Math. Model. 89 (2021) 1747–1763, https://doi.org/10.1016/j.apm.2020.08.032.

[94] L. Bian, G. Wang, Reliability analysis for competing failure processes with mutual dependence of the system under the cumulative shock, in: 2020 Asia-Pacific International Symposium on Advanced Reliability and Maintenance Modeling (APARM), 2020, pp. 1–5, https://doi.org/10.1109/APARM49247.2020.9209572.

[95] W. Dong, S. Liu, S.J. Bae, Y. Cao, Reliability modelling for multi-component systems subject to stochastic deterioration and generalized cumulative shock damages, Reliab. Eng. Syst. Saf. 205 (2021) 107260, https://doi.org/10.1016/j.ress.2020.107260.

[96] Z. Fan, X. Chen, Y. Liu, F. Huang, Y. Jiang, S. Zhang, Y. Wang, Reliability research of TSV micro structure under thermal and vibration coupled load, in: 2019 Prognostics and System Health Management Conference (PHM-Qingdao), 2019, pp. 1–7, https://doi.org/10.1109/PHM-Qingdao46334.2019.8942986.

[97] Z. Fan, Y. Liu, X. Chen, Y. Jiang, S. Zhang, Y. Wang, Research on fatigue of TSV-Cu under thermal and vibration coupled load based on numerical analysis, Microelectron. Reliab. 106 (2020) 113590, https://doi.org/10.1016/j.microrel.2020.113590.